Plasma Membrane Integrity During Cell–Cell Fusion and in Response to Pore-Forming Drugs Is Promoted by the Penta-EF-Hand Protein PEF1 in *Neurospora crassa*

Marcel René Schumann, Ulrike Brandt, Christian Adis, Lisa Hartung,[1] and André Fleißner[2]
Institut für Genetik, Technische Universität Braunschweig, 38106, Germany

ABSTRACT Plasma membrane damage commonly occurs during cellular growth and development. To counteract these potentially lethal injuries, membrane repair mechanisms have evolved, which promote the integrity of the lipid bilayer. Although the membrane of fungi is the target of important clinical drugs and agricultural fungicides, the molecular mechanisms which mediate membrane repair in these organisms remain elusive. Here we identify the penta-EF-hand protein PEF1 of the genetic model fungus *Neurospora crassa* as part of a cellular response mechanism against different types of membrane injury. Deletion of the *pef1* gene in the wild type and different lysis-prone gene knockout mutants revealed a function of the protein in maintaining cell integrity during cell–cell fusion and in the presence of pore-forming drugs, such as the plant defense compound tomatine. By fluorescence and live-cell imaging we show that green fluorescent protein (GFP)-tagged PEF1 accumulates at the sites of membrane injury in a Ca^{2+}-dependent manner. Site-directed mutagenesis identified Ca^{2+}-binding domains essential for the spatial dynamics and function of the protein. In addition, the subcellular localization of PEF1 revealed that the syncytial fungal colony undergoes compartmentation in response to antifungal treatment. We propose that plasma membrane repair in fungi constitutes an additional line of defense against membrane-disturbing drugs, thereby expanding the current model of fungal drug resistance mechanisms.

KEYWORDS membrane repair; penta-EF-hand protein; cell fusion; *Neurospora crassa*; antifungal drug

THE plasma membrane of any living cell constitutes the prime barrier between the cytosol and the outer environment. It controls the import and export of ions and molecules, thereby establishing chemical and electrical gradients required for normal physiological functioning. Membrane disintegration destroys this selective permeability, allows the mixture of inner and outer constituents and ultimately results in cell death. While membrane integrity is essential for cell survival, damage of this outer barrier frequently occurs in all organisms during physiological or pathophysiological conditions (Horn and Jaiswal 2018; Nakamura *et al.* 2018). Most common causes of membrane rupture include mechanical shear stress or exposure to pore-forming drugs. For example, cells in mechanically active tissue, such as mammalian skeletal and cardiac muscle, frequently encounter membrane rupture through physical force (McNeil and Khakee 1992; Clarke *et al.* 1995). Similarly, cells undergoing sexual or somatic fusion are at risk of rupture during plasma membrane merger as observed in yeast or filamentous fungi (Jin *et al.* 2004; Palma-Guerrero *et al.* 2014). Mounting evidence also points to important roles of membrane damage during various pathophysiological conditions including muscular dystrophies, diabetes, or ischemia-reperfusion injuries associated with strokes or heart attacks (Howard *et al.* 2011; Tzeng *et al.* 2014; Barthélémy *et al.* 2018). Membrane disruption by pore-forming drugs is common in host–pathogen interactions, where the cellular armory involves attack or defense compounds, such as plant saponins, which target the membrane and cause its disintegration (Dal Peraro and van der Goot 2016; Mondal *et al.* 2018). The saponin tomatine, for example, belongs to the group of steroidal glycoalkaloids

doi: https://doi.org/10.1534/genetics.119.302363
Manuscript received March 28, 2019; accepted for publication June 14, 2019; published Early Online July 3, 2019.
Supplemental material available at Figshare: https://doi.org/10.25386/genetics.8239490.
[1]Present address: Institut für Pflanzengenetik, Leibniz Universität Hannover, Herrenhäuser Str. 2, 30419 Hannover, Germany.
[2]Corresponding author: Institut für Genetik, Technische Universität Braunschweig, Spielmannstraße 7, 38106 Braunschweig, Germany. E-mail: a.fleissner@tu-bs.de

and is produced by *Solanum* species, such as tomato (*Solanum lycopersicum*), as a preformed defense compound against fungal infections (Friedman 2002). In clinic and in agriculture, pore-forming drugs also represent important weapons for fighting pathogenic microbes. Examples include the polyene antibiotics for treating fungal infections of human, animals and plants (Bolard 1986; Chandrasekar 2011).

To survive membrane damage, cells must quickly and efficiently reseal the wounded area and restore the preinjury state. Depending on the size and nature of the injury, different repair mechanisms are employed, including the formation of membrane patches, removal of the injured area by exo- and/or endocytosis, membrane blebbing, and closing of the wound by clotting (Horn and Jaiswal 2018; Nakamura *et al.* 2018). Membrane patches, which allow the repair of larger wounds such as ruptures, are formed via the fusion of vesicles which accumulate in masses at the injured side followed by merger of the patch with the plasma membrane (McNeil and Kirchhausen 2005; Davenport and Bement 2016). Endo- and exocytosis remove the damaged area by internalization or detachment and efficiently repair pore-like injuries (Idone *et al.* 2008a,b). The exocytosis of internal membrane structures also releases plasma membrane tension, which promotes spontaneous sealing of small injuries. This process can be furthered by the disassembly of the underlying cortical cytoskeleton, resulting in tension relief (Togo *et al.* 2000). Membrane blebbing involves protruding of the injured membrane from the cell body followed by shedding of the damaged section (Babiychuk *et al.* 2011). Clotting, finally, describes a colloidal reaction of the protoplasm, in which similar to blood clotting, proteins, organelles, and/or vesicles aggregate into three-dimensional structures, which can plug larger wounds and prevent cytoplasmic loss even before the plasma membrane has been reconstituted (Eddleman *et al.* 2000; Horn and Jaiswal 2018).

While these different repair mechanisms vary in their underlying principles, they all depend on factors and structures present in the cell before injury occurrence. Membrane damage always threatens the survival of the cell and necessitates responses faster than the *de novo* synthesis of proteins. Immediate sensing and localization of an injury therefore represents the first and foremost step of any membrane repair system. A conserved trigger of plasma membrane repair mechanisms is the influx of Ca^{2+} ions through the wound into the cell. Intact cells usually maintain a Ca^{2+} gradient across their plasma membrane, with the external concentration exceeding the internal one. The rapidly increasing internal Ca^{2+} concentration after injury is detected by Ca^{2+}-responsive proteins, which function as sensors within the repair machinery (Horn and Jaiswal 2018; Nakamura *et al.* 2018). In animal cells, for example, the Ca^{2+}-binding penta-EF-hand protein ALG-2 (apoptosis-linked gene-2) initiates the accumulation of ALG-2-interacting protein X (ALIX), and the ESCRT-III and Vps4 complex at the injured cell membrane, resulting in cell recovery by shedding of the damaged site (Scheffer *et al.* 2014; la Cour *et al.* 2018).

So far, membrane repair mechanisms have mostly been studied in animal cells. Besides hints to conserved functions of individual factors, such as synaptotagmins, in plants, animals, and fungi (Aguilar *et al.* 2007; Schapire *et al.* 2009), it remains unclear if the broader repair machineries are conserved throughout the different kingdoms. In recent years, the filamentous fungus *Neurospora crassa* has advanced as an attractive model organism for studying general eukaryotic and specifically fungal cell biology. Topics addressed in this experimental system include cell polarity, directed growth, signal transduction, and cell–cell fusion (Riquelme *et al.* 2011; Daskalov *et al.* 2016). Earlier studies reported different types of membrane damage occurring in this fungus. First, as many fungi, *N. crassa* is inhibited by polyene antibiotics, such as nystatin, which induce pore formation in the plasma membrane (Kinsky 1961). Second, during colony establishment of this fungus, germinating vegetative spores, so-called conidia, undergo fusion to form a supracellular unit, which further develops into the mycelial colony. These fusion events bear the risk of lysis, especially in strains exhibiting aberrant cell–cell fusion, such as the Δ*Prm1* mutants of *Saccharomyces cerevisiae* or *N. crassa* (Jin *et al.* 2004; Palma-Guerrero *et al.* 2014). The PRM1 protein possesses a conserved function in fungal cell–cell fusion, and its absence results in fusion failure of ∼50% of fusion pairs and increased cell lysis (Heiman and Walter 2000; Fleissner *et al.* 2009; Palma-Guerrero *et al.* 2014). Time-lapse microscopy of mating between Δ*Prm1* mutant cells of baker's yeast revealed a strong correlation between membrane merger and cell lysis, suggesting that lysis was the consequence of membrane rupture during engagement of the cell fusion machinery (Jin *et al.* 2004; Aguilar *et al.* 2007). A third type of membrane injury occurs in mature colonies of *N. crassa*. The fungus grows as a syncytial network of filament-like hyphae, which are compartmentalized by cross-walls containing a central pore. Injury of the syncytium, for example by the transsection of hyphae, results in clogging of the septal pore next to the injured compartment, followed by membrane sealing (Tenney *et al.* 2000; Yuan *et al.* 2003; Fleissner and Glass 2007).

In this study, we identify the ALG-2 homologous penta-EF-hand protein PEF1 as part of the cellular response to the above-described various types of membrane injury. In contrast to animal cells, this function seems to be independent of the ESCRT-III complex, suggesting a so far undescribed membrane repair mechanism involving PEF1. Interestingly, lack of the *pef1* gene results in an increased sensitivity to the pore-forming plant defense compound tomatine. We hypothesize that membrane repair might constitute a fungal defense response against membrane-disturbing drugs and might therefore also contribute to pathogenic growth and development.

Materials and Methods

N. crassa strains and growth media

Fungal strains employed in this study are listed in Table 1. Strains were cultivated on Vogel's minimal medium (MM) (Vogel 1956) supplemented with 2% sucrose as the carbon source and with 1.5% agar for solid media. For auxotrophic strains, the required supplements were added to MM (http://www.fgsc.net/neurospora/neurosporaprotocolguide.htm). For media lacking Ca^{2+}, $CaCl_2$ was omitted from MM, and agarose was used instead of agar for solidifying the medium. If not indicated otherwise, cultures were incubated at 30°.

Gene deletion mutants used in this study were obtained from the Neurospora gene knockout collection (Dunlap *et al.* 2007), provided by the Fungal Genetics Stock Center (FGSC).

To generate double mutants, crosses were performed on Westergaard's medium as described earlier (Westergaard and Mitchell 1947). To test the mating type of progeny, strains were crossed with the reference strains FGSC 2489 and FGSC 988.

Plasmid construction

To tag PEF1 with the green fluorescent protein (GFP), the *pef1* open reading frame was amplified by PCR using primers 356 and 357 (Supplemental Material, Table S1). The obtained fragment was cloned into the expression plasmid pMF272, which contains the overexpression promoter *Pccg-1* (Freitag *et al.* 2004), through the restriction sites *Xba*I and *Pac*I. The resulting plasmid was integrated into the *his-3* locus of strain GN2-50 (Δ*pef1*, *his-3*$^-$). To express the *pef1-gfp* construct under control of the native promoter, the *pef1* open reading frame plus a 1-kb fragment upstream of the start codon was amplified by PCR with primers 633 and 357. The obtained fragment was cloned through the *Not*I and *Pac*I restriction sites into pMF272, resulting in replacement of the *Pccg-1* promoter by the *Ppef1-pef* fragment. The resulting construct was also integrated at the *his-3* locus of strain GN2-50.

To tag the ESCRT-III complex proteins CHMP1 and SEC-31 with GFP, the *chmp1* open reading frame was PCR amplified using primers 1106 and 1107, and the *sec-31* open reading frame by primers 1110 and 1111. Both fragments were cloned individually into plasmid pMF272 via the *Xba*I and *Pac*I restriction sites. The resulting plasmids were integrated at the *his-3* locus of strain FGSC 6103 (*his-3*$^-$).

To obtain *pef1* expression constructs carrying point mutations in the EF-1 or EF-3 domain encoding regions, the *pef1* open reading frame was amplified as two fragments to introduce the point mutations through the primers. For the EF-1 construct primer pairs 944/598 and 597/945 were used, and for the EF-3 construct pairs 595/598 and 597/596. The fragments were assembled by yeast recombinational cloning using the yeast vector pRS426 as described in Colot *et al.* (2006). The resulting constructs were cloned into pMF272 via the *Xba*I and *Pac*I restriction sites. The final plasmids were transformed into strain GN7-50 (Δ*Prm1*, Δ*pef1*, *his-3*$^-$).

Transformation of N. crassa

N. crassa strains were transformed by electroporation of macroconidia according to an earlier described protocol (Margolin *et al.* 1997).

Phenotypical analysis of aerial hyphal growth, growth rate, and sporulation

The growth rate of aerial hyphae was determined by inoculating 2 ml of liquid MM with 3×10^6 conidia. The culture tubes were incubated for 5 days in complete darkness at 30°. For each strain four replicates were measured.

To address linear hyphal growth, race tubes containing 12 ml of solid MM were inoculated with 3×10^6 conidia. The linear growth was measured from 24 to 72 hr at 25° in constant light. For each strain, four replicates were tested.

For determining macroconidia production, slant tubes with 3 ml solid MM were inoculated with 3×10^6 conidia. The cultures were incubated for 3 days at 30° in the dark and for 4 more days at room temperature in daylight conditions. The conidia were harvested by vortexing the slant tube with 2 ml ddH_2O, and hyphal fragments were removed by filtering through cheesecloth. The number of conidia from four independent replicates was counted for each strain.

Sample preparation for microscopy and quantitative germling fusion assay

To quantify fusion and lysis rates, 3×10^6 spores were plated on solid MM in 9-cm Petri dishes. Cultures were incubated for 4 hr at 30°. Squares of agar measuring 1 cm^2 were excised and observed on a Zeiss Observer 2.1 microscope using Nomarski optics with a Plan-Neofluar 100×/1.30 oil immersion objective (420493-9900). Cell lysis was apparent by strong vacuolization of the germlings (Palma-Guerrero *et al.* 2014). For microscopy of hyphae, cultures were grown overnight at 30°. One square centimeter agar squares were cut from the edge of the colony where hyphal density was low and analyzed by microscopy as described above.

Live-cell imaging and fluorescence microscopy were conducted as described earlier (Serrano *et al.* 2018).

To analyze PEF1-GFP recruitment in response to the antifungal drugs nystatin and tomatine, germlings were incubated as mentioned above. Five microliters of 0.1 mg/ml nystatin (CAS-Nr. [1400-61-9]) and 2 mg/ml tomatine (CAS-Nr. [17406-45-0]) solutions (diluted in DMSO) were added directly on top of the agar slides and incubated for up to 5 min before analysis by Nomarski and fluorescent microscopy. For quantitative assays, 100 lysed germlings were tested for PEF1-GFP recruitment. Each test was independently repeated two more times.

For time-lapse microscopy of PEF1 recruitment in response to nystatin, 5×10^5 spores were incubated in 200 μl of liquid MM in ibidi eight-well μ-slides (www.ibidi.com, ordering number 80826) for 3 hr at 30°. After imaging of the untreated

Table. 1 Strains used in this study.

Strain	Genotype	Origin of reference
A29	*matA, Prm1::hph*	Fleissner et al., 2009
A32	*mata, Prm1::hph*	Fleissner et al., 2009
C9-15	*matA, het-c2 pin-c2 thr2*	Xiang and Glass, 2002
CR73-1	*mata, his-3::Pccg1-h1-dsRed*	Rasmussen et al., 2008
FGSC 988	*mata*	FGSC
FGSC 2489	*matA*	FGSC
FGSC 6103	*matA, his-*	FGSC
FGSC15890	*mata, pef1::hph*	FGSC
FGSC17273	*mata, fig-1::hph*	FGSC
FGSC19267	*mata, lfd-2::hph*	FGSC
GN2-50	*mata ,pef1::hph, his-*	This study
GN2-78	*matA, his-3::dsRed-hex1*	This study
GN3-9	*matA, Prm1::hph, his-3::Pccg-1-pef1-gfp*	This study
GN3-17	*mata, pef1::hph, his-3::Pccg1 pef1-gfp*	This study
GN3-36	*matA, het-c1, pin-c1, his-3::Pccg-1-pef1-gfp, pyr4*	This study
GN6-42	*mata, Prm1::hph syt-1::hph*	This study
GN6-47	*matA, pef1::hph syt-1::hph*	This study
GN6-48	*matA, Prm1::hph pef1::hph syt-1::hph*	This study
GN6-62	*matA,his-3::Pccg-1-syt-1-mcherry*	This study
GN7-50	*mata, Prm1::hph, pef1::hph, his-*	This study
GN7-54	*mata, Prm1::hph, pef1::hph, his-3:Pccg-1 pef1-gfp*	This study
GN8-76	*matA, pef1::hph fig-1::hph*	This study
GN8-80	*matA, pef1::hph lfd-2::hph*	This study
GN9-1	*mata, Prm1::hph pef1::hph his-3::Pccg-1-pef1 E233A- gfp*	This study
GN9-3	*mata, pef1::hph his-3::Ppef1-pef1-gfp*	This study
GN9-22	*matA, pef1::hph his-3::Ptef-1-pef1-gfp*	This study
GN9-34	*mata, Prm1::hph pef1::hph his-3::Pccg-1-pef1 E164A, E166A-gfp*	This study
GN9-48	*matA, his-3::Pccg-1 sec-31-gfp*	This study
GN9-50	*matA, his-3::Pccg1 chmp-1-gfp*	This study
GN10-10	*mata, pef1::hph lfd-1::hph*	This study
JPG6	*mata, lfd-1::hph*	Palma-Guerrero et al., 2015
N5-20	*mata Prm1::hph pef1::hph*	This study
S10	*matA, trp-1 his-3::Pccg-1-pef1-gfp*	This study
S20	*matA, nic-3 his-3:Pccg1-dsRed-hex-1*	This study
S48	*matA, hex-1::hph his-3::Pccg1-pef1-gfp*	This study

FGSC, Fungal Genetics Stock Center.

cells, 30 μl of a 0.1 mg/ml nystatin solution was carefully added to the side of the chamber to avoid movement of the germlings. Cells were further imaged by fluorescence microscopy.

Analysis of septal pore plugging

To analyze PEF1 recruitment to the septal plug and to quantify septal plugging, the fungus was cultivated as described above for the microscopy of hyphae. To cut the hyphae, a laser microdissection system (CellCut Plus System, Molecular Machines and Industries) equipped with a UV laser (355 nm) and combined with an Olympus IX81 microscope was used. In quantitative assays, which did not require the direct observation of the injury occurrence, hyphae were cut with a razor blade and imaged with the above-described Zeiss Observer 2.1 microscope set up.

Analysis of PEF1 localization during vegetative incompatibility

Incompatible heterokaryons between strains GN3-36 and C9-15 were formed and analyzed as described earlier (Fleissner and Glass 2007). In brief, spores of the two auxotrophic strains were mixed and plated on MM, allowing only the growth of heterokaryotic colonies. The culture medium contained 0.003% methylene blue to stain dead hyphal compartments indicating the activation of programmed cell death. Septa delimiting dead compartments were analyzed for PEF1 accumulation by fluorescence microscopy.

Stress tests

To test the sensitivity of *N. crassa* strains to EGTA, SDS, nystatin, and tomatine, spore serial dilution assays were conducted. To restrict hyphal growth and promote the formation of individual, distinct colonies, BDES medium was used (Brockman and De Serres 1963). A serial dilution of 10^5–10^1 spores were spotted in 5-μl droplets on BDES plates. Cultures were incubated for 2–3 days at 30°, and growth of the reference strain and the mutants was compared.

Data availability

All strains and plasmids are available on request. We confirm that all data and information necessary to confirm the conclusions of this study are present in the article, figures, tables, and supplemental material. Supplemental material available at Figshare: https://doi.org/10.25386/genetics.8239490.

Results

The N. crassa penta EF-Hand protein PEF1 is dispensable for vegetative growth and cell–cell fusion

The original motivation of this study was not to identify membrane repair mechanisms in *N. crassa*, but to find Ca^{2+}-responsive proteins potentially involved in signaling processes mediating vegetative cell–cell fusion, since earlier studies revealed that Ca^{2+} is essential for this process (Palma-Guerrero *et al.* 2013). As one candidate, the penta EF-Hand protein PEF1 (NCU02738) was chosen. An earlier study described PEF1 as the only homolog of animal ALG-2. Its role and function in fungal growth and development remained, however, unknown (Cano-Domínguez *et al.* 2008).

The predicted *N. crassa pef1* encoding open reading frame consists of 1266 bp and contains three introns, whose positions were confirmed by complementary DNA (cDNA) sequencing. The gene encodes a protein of 311 amino acid residues, with a predicted molecular weight of 35,581 Da (http://fungidb.org). Sequence comparison by BLAST analysis revealed that the N-terminal third of the protein (aa 1–111) is not conserved outside the taxon fungi, while the N-terminal two-thirds (aa 112–311), including the five putative calcium-binding EF domains, show high conservation (*e.g.*, 44% identity to ALG-2 of *Mus musculus*).

To test the role of PEF1 for the growth and development and specifically vegetative cell–cell fusion of *N. crassa*, we obtained the Δ*pef1* gene deletion strain FGSC 15890 from the *N. crassa* gene knockout collection (Dunlap *et al.* 2007) and verified the integration of the gene replacement cassette at the *pef1* locus by PCR analysis using primers 317 and 374 (data not shown). Compared to the wild-type reference strain, the mutant shows normal hyphal growth and formation of aerial hyphae (Figure S1, A and B), indicating that PEF1 is dispensable for general vegetative growth. It produces, however, significantly higher numbers of vegetative spores (Figure S1C), confirming the observations made for an independently constructed Δ*pef1* mutant analyzed in an earlier study (Cano-Domínguez *et al.* 2008). The only macroscopically discernable difference between the wild type and Δ*pef1* is a dark pigmentation occurring robustly between the mycelia and the glass surface of the culture tubes (Figure S1D). This phenotype is reminiscent of the Δ*hex-1* mutant of *N. crassa*, which is unable to seal the cross-walls of its syncytial hyphae after injury, resulting in cytoplasmic leakage indicated by the brown pigmentation of mutant cultures (Jedd and Chua 2000). The extent of cytoplasmic leakage can be measured by the amount of extracellular protein, which can be recovered from the culture. When tested, however, the amount of protein obtained from wild-type and Δ*pef1* cultures was comparable, indicating that the observed pigmentation is not caused by cytoplasmic leakage (Figure S1D).

Consistent with the overall lack of growth defects, the absence of PEF1 did not affect the tropic interaction of germinating spores resulting in cell–cell fusion, indicating that PEF1 is dispensable for this process (Figure S1E).

PEF1 accumulates at the fusion point of lysing cell–cell fusion pairs

To test a potential nonessential contribution of PEF1 to the process of germling fusion during colony establishment, we tagged the protein with GFP to determine its subcellular localization. The *gfp*-encoding DNA sequence was fused to the 3′ end of the *pef1* open reading frame. This fusion construct was expressed under control of the native *pef1* promoter and alternatively under control of the overexpression promoters *Pccg-1* and *Ptef-1*, which are routinely used in protein localization studies in *N. crassa* (Freitag *et al.* 2004; Berepiki *et al.* 2010). All constructs were transformed into the Δ*pef1* mutant strain, resulting in the isolates GN9-3, GN3-17, and GN9-22, respectively. Expression controlled by the native promoter yielded no discernable fluorescence above the level of autofluorescence of the cells, suggesting that *pef1* is expressed at low levels. In contrast, germlings and growing mature hyphae of the two overexpressing strains exhibited comparable cytoplasmic fluorescence with sometimes increased signal intensity around nuclei (Figure 1 and Figure S2). The presence of GFP at the C-terminus of PEF1 did not affect the function of the protein, indicated by the complementation of the above-described hyper-sporulation phenotype of the Δ*pef1* mutant (Figure S1C). To test the dynamics of PEF1-GFP during germling fusion, spores of strains GN3-17 (*Pccg-1-pef-1-gfp*) and GN9-22 (*Ptef-1-pef-1-gfp*) were plated on MM agar plates, incubated for 3 to 4 hr at 30°, and analyzed by fluorescence microscopy. At this time point, the majority of spore germlings were undergoing pairwise interactions, indicated by the mutual attraction of germ tubes, or cell pairs were already merged. Also, networks of more than two cells formed by successive fusion events were readily observed. In the vast majority of growing, fusing, and fused cells no altered or specific localization pattern of PEF1 was observed, supporting the notion that PEF1 seems not to be involved in these processes (Figure 2 and data not shown). In rare cases, however, the PEF1-GFP signal clearly and strongly accumulated at the contact point of cell pairs (Figure 2). Interestingly, DIC imaging revealed that in these pairings the cells appeared highly vacuolized, which earlier studies identified as an indication of cell lysis (Palma-Guerrero *et al.* 2014, 2015). Live-cell imaging supported this finding, showing rapid vacuolization of some fusion pairs minutes after cell–cell contact, consistent with fusion-induced cell lysis (Figure 2). To corroborate the potential correlation between fusion pair lysis and PEF1 recruitment to the contact zone, the lysed cell pairs within the cell population were quantified and tested for PEF1-GFP presence at the fusion point. As a result, ∼1% of all formed cell pairs exhibited lysis, and ca. 90% of these lysed fusion pairings showed PEF1 recruitment to the cell–cell contact zone (Figure 2). Based on this strong correlation, we hypothesized that PEF1 is recruited to the cell–cell fusion point in response to aberrant

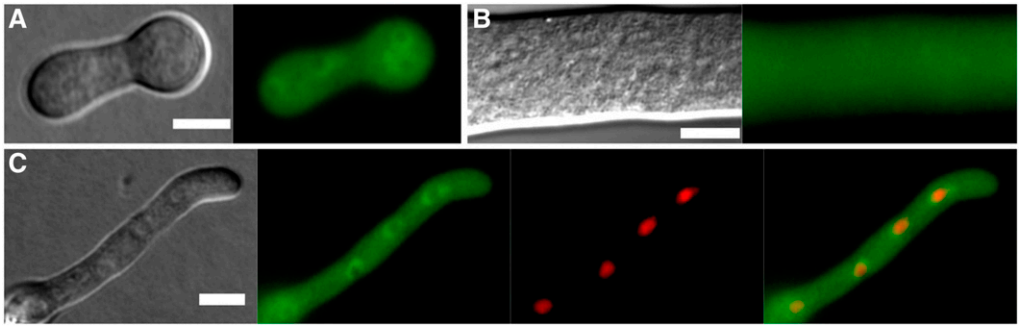

Figure 1 PEF1-GFP is a cytoplasmic protein. Subcellular localization of PEF1-GFP in germlings (A) and hyphae (B) of strain GN9-22 (*Ptef-1-pef-1-gfp*). Left: DIC image; right: GFP fluorescence image. (C) Heterokaryon of strains GN9-22 expressing *pef1-gfp* and CR73-1 expressing the nuclear marker H1-dsRed. From the left: (1) DIC, (2) GFP fluorescence, (3) dsREd fluorescence, and (4) merged image of 2 and 3. Bar, 5 μm (A and C) and 10 μm (B).

plasma membrane merger resulting in cell rupture. Since in the observed PEF1-GFP aggregates the protein is concentrated, we revisited the isolate expressing *pef1-gfp* under control of the native promoter. However, still no discernable GFP signal was detected.

To further corroborate the correlation between cell lysis and PEF1 aggregation, we expressed PEF1-GFP (from construct *Pccg-1-pef-1-gfp*) in the Δ*Prm1* mutant, which is prone to fusion-induced cell lysis. In this mutant ca. 50% of germling pairs fail to fuse their plasma membranes, and ∼10% of cell pairs undergo cell lysis (Fleissner *et al.* 2009; Palma-Guerrero *et al.* 2014). We hypothesized that the majority of these lysed cell pairs would also exhibit PEF1-GFP accumulation at the fusion point. This expectation was fully met with ∼90% of lysed cell pairs exhibiting an increased GFP signal at the cell contact zone. Although the overall number of lysed pairs was significantly higher in Δ*Prm1* than in the wild-type background, the correlation between lysis and PEF1-GFP recruitment was comparable (Figure 2D).

The lack of PEF1 results in increased lysis rates in lysis-prone mutants

To test if the observed accumulation of PEF1 at the contact point of lysing fusion pairs represents a functional response to cell injury, we compared the lysis rates of the wild type and the Δ*Prm1* mutant to those of the Δ*pef1* strain and the Δ*Prm1/*Δ*pef1* double mutant. While the frequency of fusion-induced lysis was comparable between wild type and Δ*pef1*, the lysis rate of Δ*Prm1/*Δ*pef1* doubled compared to the Δ*Prm1* single mutant. This increase could be reversed by the expression of *Pccg-1-pef-1-gfp* in the double mutant (Figure 3). Together, these data indicate that PEF1 is dispensable in the wild type but significantly promotes cell survival in the lysis-prone Δ*Prm1* mutant. Earlier studies revealed that a reduction of Ca^{2+} in the growth medium increases the lysis rates of fusion pairs in *N. crassa* and *S. cerevisiae*, leading to the hypothesis that Ca^{2+}-mediated membrane repair mechanisms counteract the effect of a lack of PRM1 (Palma-Guerrero *et al.* 2014) (Aguilar *et al.* 2007). We therefore hypothesized that PEF1 is part of this proposed membrane repair mechanism. To test this idea, we compared the lysis rates of the different isolates on standard growth medium and on medium containing only 50% of the usual Ca^{2+} [on medium with zero Ca^{2+}, cell–cell interactions and fusion are not observed and fusion-induced lysis cannot be tested (Palma-Guerrero *et al.* 2013)]. While in the wild type and the Δ*pef1* mutant the reduced Ca^{2+} had no significant effect, the lysis rate of Δ*Prm1* increased to the level observed in the Δ*Prm1/*Δ*pef1* double mutant on standard medium, indicating that either deleting *pef1* or reducing the extracellular Ca^{2+} amount had similar effects. However, the Δ*Prm1/*Δ*pef1* double mutant also exhibited a further significant increase in lysis on Ca^{2+}-reduced medium compared to standard growth conditions, suggesting that additional PEF1-independent Ca^{2+}-mediated repair mechanisms exist (Figure 3).

In addition to PRM1, earlier studies identified three additional factors, whose absence results in aberrant fusion and increased lysis rates during germling fusion, LFD-1, LFD-2, and FIG1 (Palma-Guerrero *et al.* 2014, 2015). To test if the observed role of PEF1 is specific for Δ*Prm1*-caused defects or if it is of broader significance, we introduced the Δ*pef1* gene knockout into the Δ*lfd-1*, Δ*lfd-2* and Δfig1 mutants and compared the lysis rates of the single and the respective double mutants on standard and Ca^{2+}-reduced growth medium. The lack of PEF1 resulted in increased lysis rates in all double mutants compared to the single mutants (Figure 4A). Interestingly, similar to the observation made for the Δ*Prm1* and Δ*Prm1/*Δ*pef1* mutants, the Δ*lfd-1/*Δ*pef1* and Δ*lfd-2/*Δ*pef1* double mutants exhibited similar lysis rates on standard medium to the single mutants under Ca^{2+}-reduced conditions. Again, the reduction of Ca^{2+} also further increased the frequency of lysis in the double mutants. In contrast, while deletion of *pef1* in Δfig1 significantly increased the occurrence of lysis on standard medium, the reduction of Ca^{2+} did not further increase lysis of the double mutant (Figure 4A).

The earlier study describing the role of LFD-1 also identified the synaptotagmin SYT1 as a potential mediator of plasma membrane repair. Deletion of *syt1* in Δ*Prm1* resulted in a significant increase in lysed cell pairs, similar to our observation for *pef1* (Palma-Guerrero *et al.* 2014). To test if SYT1 and PEF1 function in a common pathway or have independent functions, we constructed a Δ*pef1/*Δ*syt1* double and a Δ*Prm1/*Δ*pef1/*Δ*syt1* triple mutant and compared the fusion pair lysis rates to those of the Δ*syt1* single and the Δ*Prm1/*

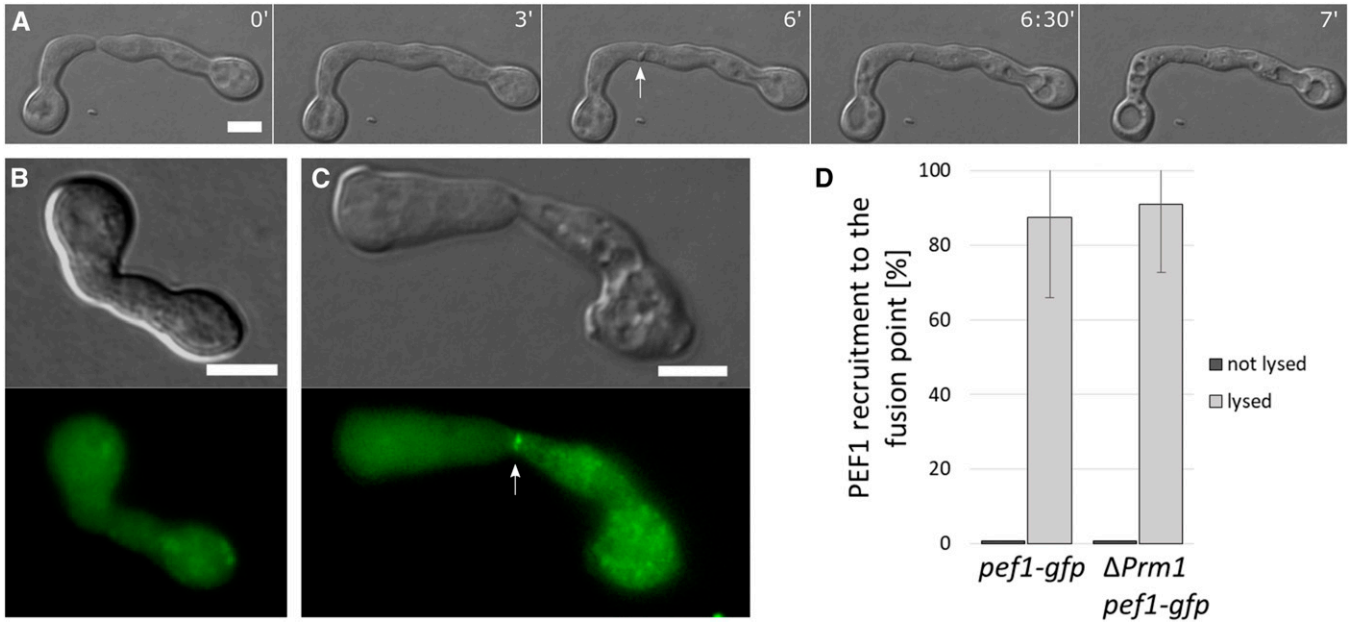

Figure 2 PEF1-GFP accumulates at the contact point of fusing cells undergoing lysis. (A) Time course of two germlings undergoing mutual attraction and fusion. At time point 6 min, note the formation of a membrane protuberance (arrow) followed by rapid vacuolization of both fusion partners indicating lysis. Time = min. (B) PEF1-GFP localization during successful cell fusion (strain GN9-22, *Ptef-1-pef-1-gfp*). (C) PEF1-GFP accumulation at the contact point of a fusion pair undergoing lysis (arrow) (strain GN9-22, *Ptef-1-pef-1-gfp*). (B and C) Top images: DIC; bottom images: GFP fluorescence. (D) Quantification of PEF1-GFP recruitment in healthy and lysed cell pairs of strains GN9-22 (Δ*pef1*, *Ptef-1-pef1-gfp*) and GN3-9 (Δ*Prm1*, *Pccg-1-pef1-gfp*). Error bars indicate the SD calculated from three independent experiments (n = 100 each). Note that while the percentage of lysed cell pairs showing PEF1-GFP accumulation at the fusion point is comparable for both strains, the overall number of lysed cell pairs is significantly higher in Δ*Prm-1* compared to the wild-type background strain (33 lysed pairs out of 300 total, compared to 8 out of 300 total, respectively). Bar, 5 μm.

Δ*syt1* double mutant. In our hands, however, the Δ*Prm1/*Δ*syt1* mutant did not exhibit increased lysis compared to Δ*Prm1*. Consistent with this finding, the triple mutant also behaved comparably to the Δ*Prm1/Δpef1* double mutant (Figure 4B). Thus, under our test conditions, SYT1 seems to make no contribution to plasma membrane integrity during germling fusion.

PEF1 is recruited to the plasma membrane in response to the action of pore-forming drugs

Cell lysis observed during aberrant plasma membrane fusion events is likely caused by membrane rupture. To investigate if PEF1 is also involved in the response to other types of membrane injuries, we sought different ways of harming the fungal plasma membrane. Most fungi, including *N. crassa*, are sensitive to polyene antibiotics, which bind to ergosterol in the plasma membrane, resulting in pore formation. The polyene nystatin is an important antifungal drug, which is commonly used to treat human fungal infections caused by *Candida* or *Aspergillus* species (Semis *et al.* 2010). One consequence of the exposure to nystatin is an increased Ca^{2+} influx into the cell (Eilam and Grossowicz 1982). To test the effect of nystatin, 3-hr-old spore germlings of the PEF1-GFP expressing strain GN9-22 (*Ptef-1-pef1-gfp*) were analyzed by light and fluorescence microscopy. Before the addition of nystatin, germlings had a healthy appearance and exhibited the typical cytoplasmic PEF1-GFP signal (Figure 5A). Within 40 sec after the addition of nystatin, cells became vacuolized, indicating lysis, and PEF1-GFP accumulated in puncta at the plasma membrane. Consistent with an enrichment of the nystatin target ergosterol at the growing cell tips, the GFP signal was also most apparent at this cellular region, where its intensity increased over time (Figure 5B). Quantification experiments revealed that this recruitment occurred in basically every germling. In growth medium, containing no Ca^{2+}, this number was reduced by ~30%, suggesting that extracellular Ca^{2+} is required for efficient PEF1 recruitment to the plasma membrane (Figure 5C).

To corroborate the observed response of PEF1 to pore-inducing drugs, we also tested the subcellular protein dynamics during treatment with the plant defense compound tomatine. Similar to the polyenes, tomatine binds ergosterol resulting in pore formation. Administering tomatine to 3-hr-old germlings of strain GN9-22 (*Ptef-1-pef-1-gfp*) resulted in cell lysis and accumulation of PEF1 at the plasma membrane, similar to the observations made for nystatin (Figure 6A). The signal intensity observed at the cell tips was, however, even more intense. Quantifications revealed PEF1 recruitment in the large majority of cells. In the absence of extracellular Ca^{2+}, this number was significantly reduced (Figure 6B). Taken together these observations indicate that PEF1 is also recruited to the plasma membrane in response to the action of pore-forming drugs.

To test if this recruitment is also observed in mature hyphae, strain GN9-22 (*Ptef-1-pef1-gfp*) was inoculated on solid MM and cultivated overnight, resulting in the formation

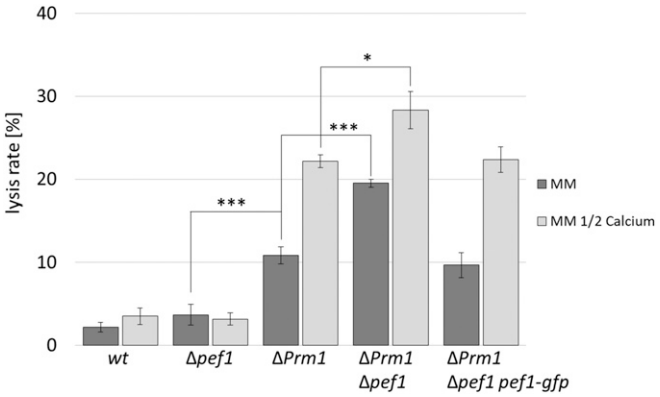

Figure 3 Lack of PEF1 increases the lysis rate during germling fusion in the lysis-prone Δ*Prm1* mutant. Quantification of the lysis rate during germling fusion of the wild-type strain (FGSC 988) compared to Δ*pef1* and Δ*Prm1* deletion and double mutants (FGSC 15890, A32, N5-20, respectively) and the complemented isolate GN7-54 (Δ*Prm1*/Δ*pef1*, *Pccg-1-pef1-gfp*). Strains were incubated on MM or MM with 50% Ca^{2+}. Error bars indicate the SD calculated from three independent experiments (n = 100 each). The asterisks represent statistically significant differences determined by the Student's t-test (*$P \leq 0.05$; ***$P \leq 0.001$).

of mature mycelial colonies. Treatment of these cultures with tomatine also resulted in a rapid accumulation of PEF1-GFP at the majority of tips of smaller branch hyphae in the inner parts of the colony (70%, $n = 30$) (Figure 6C). Surprisingly, no recruitment was observed at the tips of big leading hyphae (0%, $n = 30$). Studies on liposomes revealed that the concentration of sterols in the membrane must exceed a certain threshold before the interaction with saponins results in complex formation (Elias *et al.* 1979). To test for the presence of sterols, we stained the different hyphal types with filipin. The results indicated that only small branch hyphae but not leading hyphae carry a sterol-rich domain at their tip (data not shown). This observation suggests that the sterol-mediated membrane disturbing action of tomatine mostly affects the smaller hyphae in the inner parts of the colony, consistent with the recruitment pattern of PEF1. Interestingly, we also observed PEF1 accumulation at the septal pores in all hyphal types (PEF1-GFP at 94% of all septa, $n = 100$), suggesting their closure by clogging (Figure 6, D and E). To corroborate this finding, we also analyzed PEF1 dynamics at septal pores after addition of nystatin. As a result, comparable recruitment to the septal pores was observed (PEF1-GFP at 95% of all septa, $n = 100$).

PEF1 is involved in septal pore sealing in response to injury and during induced cell death

In young and healthy growing hyphae, septal pores are typically open and allow the rapid exchange of cytoplasm and organelles between the hyphal compartments. In response to injury or during aging and apoptotic-like reactions the pores are closed by a clogging mechanism (Fleissner and Glass 2007). During injury, this reaction involves a specific organelle, the Woronin body, which translocates into the septal pore and becomes surrounded by aggregating proteins (Jedd and Chua 2000; Tenney *et al.* 2000; Lai *et al.* 2012). In contrast, the developmental compartmentation is Woronin body independent (Markham 1994; Fleissner and Glass 2007). To test the role of PEF1 in these different processes, we tested the PEF1-GFP localization during hyphal injury and during programmed cell death. For the former, mature hyphae of strain GN3-17 (*Pccg-1-pef1-gfp*) were cut with a UV pulse laser at a laser microdissection microscope, and the septa next to the injury were observed by fluorescence microscopy. The injured hyphae showed the typical plugging reaction, and PEF1 accumulated at the majority of closed septal pores. Chelating of Ca^{2+} by the addition of EGTA resulted in a reduced number of septa exhibiting the PEF1-GFP signal, suggesting that Ca^{2+} promotes aggregation of the protein (Figure 7, A and E). To corroborate the position of the PEF1 aggregate at the septal plug, we co-localized PEF1-GFP with the Woronin body, which was visualized by tagging its main constituent, the HEX-1 protein, with the red fluorescent protein dsRED. Co-localization of both proteins was detected (Figure 7B). To test if the PEF1-GFP accumulation at the septal plug is Woronin body dependent, the GFP fusion protein was expressed in a Δ*hex-1* mutant strain. Δ*hex-1* hyphae lack Woronin bodies, resulting in an inability to quickly seal the septal pore after injury and significant cytoplasmic leakage. However, eventually Δ*hex-1* pores also become plugged by a clogging mechanism. PEF1 was also present at these sealed septa, indicating that the PEF1 recruitment to the septal pore is Woronin body independent (Figure 7C). To test if PEF1 is required for septal sealing, the plugging efficiency of wild-type and Δ*pef1* hyphae was compared by measuring the time required for complete sealing after hyphal transsection. No differences were found indicating that PEF1 is dispensable for septal sealing. Interestingly, however, chelating of Ca^{2+} resulted in delayed plugging of septal pores in both strains, suggesting that Ca^{2+} also promotes clogging as a wound response (Figure 7F).

Hyphae of different *N. crassa* colonies are able to fuse; however, this fusion between different individuals is subject to a genetically encoded control system. Fusion between hyphae that differ in their allelic specificity of at least one of 11 heterokaryon incompatibility (het) loci results in septal pore plugging in the fused compartments and subsequent programmed cell death (Glass and Kaneko 2003). To test if PEF1 is also involved in these Woronin body-independent clogging processes, PEF1-GFP (expressed from *Pccg-1-pef1-gfp*) was localized in an incompatible heterokaryon of two strains carrying different *het-c* alleles. In these cultures, two incompatible strains with different auxotropic markers are forced into a heterokaryon. Because of their auxotrophic requirements, the strains can only grow on MM when fused, but at the same time the permanent induction of the incompatibility reaction results in high numbers of hyphal compartments undergoing programmed cell death. The obtained heterokaryons exhibited a typical incompatibility phenotype, including slow growth, complete absence of sporulation, and high numbers of dying compartments, which were visualized

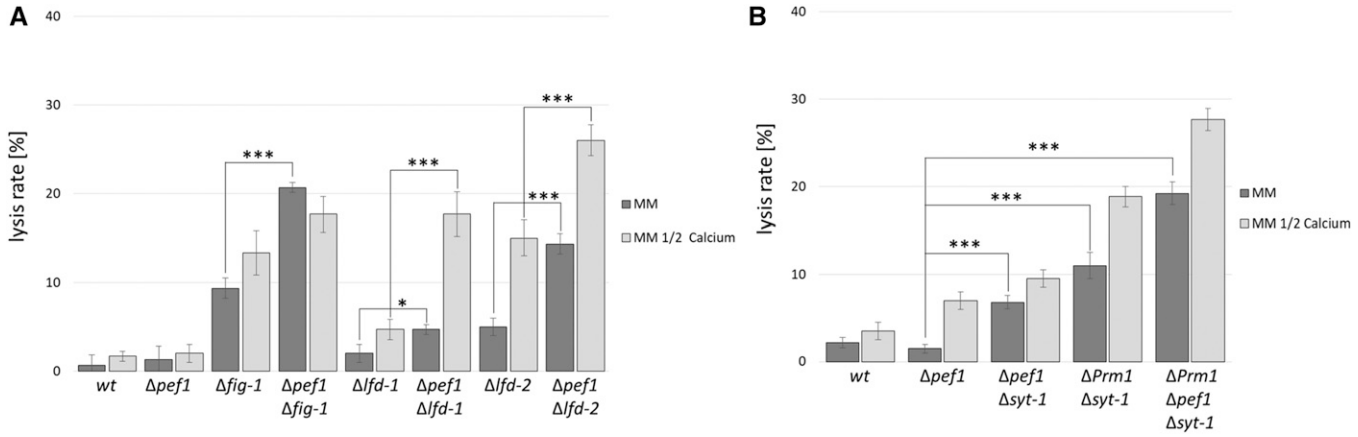

Figure 4 Lack of PEF1 increases the lysis rate in mutants with membrane merger defects. (A) Quantification of the lysis rate during germling fusion of the wild-type strain (FGSC 988) compared to Δ*pef1* (FGSC 15890), Δ*fig-1* (FGSC 17273), Δ*lfd-1* (JPG6), Δ*lfd-2* (FGSC 19267), and double mutants (GN8-76, GN10-10, GN8-80, respectively). (B) Quantification of the lysis rate during germling fusion of the wild-type strain (FGSC 988) compared to Δ*pef1* (FGSC 15890), the double mutants Δ*pef1*/Δ*syt-1* (GN6-47) and Δ*Prm1*/Δ*syt-1* (GN6-42), and the triple mutant Δ*Prm1*/Δ*pef1*/Δ*syt-1* (GN6-48). Strains were grown on MM or MM with 50% Ca^{2+}. Error bars indicate the SD calculated from three independent experiments (n = 100 each). The asterisks represent statistically significant differences determined by the Student's t-test (*$P \leq 0.05$; ***$P \leq 0.001$).

by methylene blue staining. PEF1-GFP was readily observed at the plugged septa of compartments undergoing cell death, indicating that it is also involved in this clogging mechanism (Figure 7D).

PEF1 promotes resistance against the phytoanticipine tomatine

Based on the observed translocation of PEF1 to the plasma membrane in response to pore-forming drugs, we hypothesized that PEF1 promotes resistance against these substances. In addition, an earlier study described that mutants of *S. cerevisiae* lacking the *pef1* homologous gene exhibit growth defects on medium containing SDS or EGTA (Vernarecci *et al.* 2007). We therefore compared growth of the wild type, the Δ*pef1* mutant, and the Δ*pef1* mutant expressing the functional PEF1-GFP fusion protein (expressed from *Ptef-1-pef1-gfp*) on medium containing nystatin, tomatin, SDS, and EGTA. While no growth differences between the tested strains were detected on nystatin, SDS, and EGTA, growth of the Δ*pef1* mutant was significantly reduced on the plant saponin tomatine, suggesting that PEF1 contributes to the stress response against this pore-forming drug (Figure 6F and Figure S3).

The EF-hand domains are essential for PEF1 function

The reduced PEF1 plasma membrane recruitment in response to lysis on medium with reduced amounts of Ca^{2+} suggested a role of binding to Ca^{2+} in the protein dynamics. We therefore hypothesized that the mutation of Ca^{2+}-binding domains would also result in reduced or absent membrane recruitment of the protein. Members of the PEF protein family contain five conserved EF-hand domains comprising helix–loop–helix Ca^{2+}-binding motifs, which exhibit different Ca^{2+}-binding affinities. In *S. cerevisiae* the EF-1-hand and EF-3-hand domains of the PEF1 homologous Pef1p possess the highest affinity to Ca^{2+} (Vernarecci *et al.* 2007). To test the role of these conserved domains for PEF1 of *N. crassa*, we introduced E164A, E166A mutations into EF-1 and in an independent construct an E233A change into EF-3 (Figure 8A). Both mutated gene constructs were fused with *gfp* and were expressed in the Δ*Prm1*/Δ*pef1* double mutant under control of the *ccg-1* promoter. The subcellular dynamics of both variants were compared to wild-type PEF1-GFP in healthy spore germlings and during drug-induced and fusion-induced cell lysis. The overall signal intensity was comparable in all strains indicating that the mutations had no negative effect on transcription, translation, or protein stability. In the absence of the pore-forming drugs and in healthy fusing germlings, no differences were observed for the three protein variants, and all showed the typical cytoplasmic localization (Figure 8). In contrast, after treatment with nystatin, wild-type PEF1 accumulated at the plasma membrane in the above-described manner, while no membrane recruitment was observed for the mutated variant. Similarly, the mutated proteins did not accumulate at the contact point of lysing fusion pairs (Figure 8). Consistent with these findings, the mutated variants did not complement the increased lysis rates of fusing Δ*Prm1*/Δ*pef1* germlings (Figure 8B). Taken together, these data indicate that the EF-1- and the EF-3-hand domains are essential for normal PEF1 functioning, suggesting that Ca^{2+} binding is mediating the dynamics of this protein during drug- and fusion-induced lysis.

PEF1 appears to function independently of the ESCRT complex during fusion-induced lysis

A recent study describing a role of the mammalian PEF1 homolog ALG-2 in membrane repair linked its function to the ESCRT-III complex. After laser-induced injury of the plasma membrane of myoblasts, the ESCRT complex and

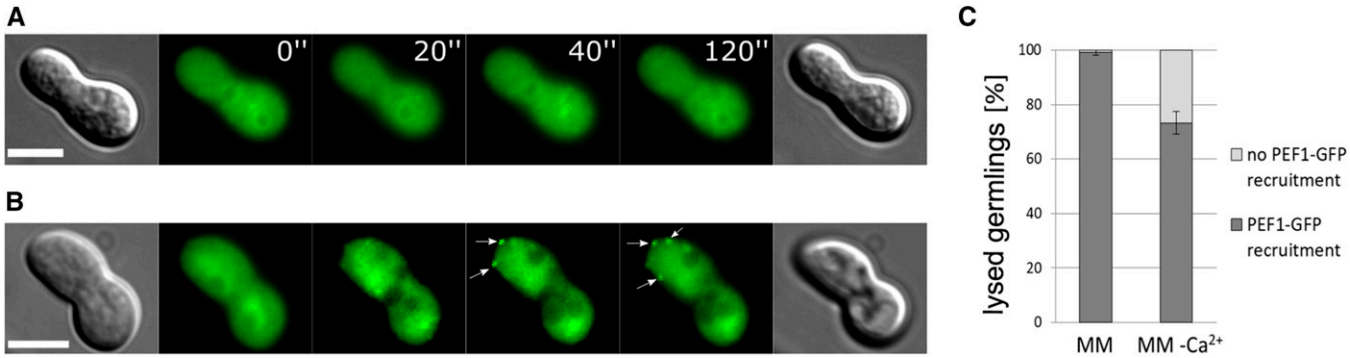

Figure 5 PEF1-GFP is recruited in response to nystatin-induced cell lysis. (A and B) Subcellular localization of PEF1-GFP in germlings of strain GN9-22 (*Ptef-1-pef-1-gfp*). (A) Control, without the addition of nystatin. (B) Nystatin was added directly after the photo for time point 0′ was taken. (A and B) DIC image on the left: 0 sec; DIC image on the right: 120 sec. Bar, 5 μm. Arrows in B indicate punctate PEF1-GFP aggregates. (C) Quantification of cells exhibiting PEF1-GFP recruitment to the plasma membrane after treatment with nystatin on MM and MM without Ca^{2+}. Error bars indicate the SD calculated from three independent experiments (n = 100 each). The asterisks represent statistically significant differences determined by the Student's t-test ($*P \leq 0.05$; $***P \leq 0.001$).

accessory proteins accumulated at the wound site in an ALG-2-dependent manner, resulting in membrane repair (Scheffer *et al.* 2014). To test if PEF1 mediates a similar process in *N. crassa*, we localized the conserved and essential ESCRT-III constituents CHMP1 and SEC31 via GFP tagging. Spores of the resulting strains, GN9-50 and GN9-48, respectively, were incubated on solid medium for 3 hr at 30°. The spore germlings showed cytoplasmic fluorescence with some increased signal intensity in dot-like structures. No accumulation of the signal at the fusion point or the plasma membrane was observed in lysed fusion pairs or after treatment with nystatin (Figure 9). Together these data suggest that unlike in mammalian cells, PEF1 is not mediating the assembly of the ESCRT complex at wound sites and might therefore mediate a different so far unknown mechanism of fungal plasma membrane repair.

Discussion

PEF1 dynamics depend on Ca^{2+}

Plasma membrane injury commonly occurs during growth and development of all organisms, posing the risk of rapid cell death. To counteract the life-threatening membrane disintegration, efficient membrane repair mechanisms have evolved, which commonly include the activity of Ca^{2+}-responsive proteins. In this study we identified the penta-EF-hand protein PEF1 as a response mediator for different types of membrane injury, including fusion-induced membrane rupture and drug-induced pore formation. Fungal PEF1 homologs consist of a conserved C-terminal part with homology to plant and animal proteins, including the mammalian ALG-2. The N-terminal third of the protein is specific for the taxon fungi, suggesting some fungal-specific function. Similar to ALG-2 in mammals, PEF1 rapidly translocates to the plasma membrane after injury in a Ca^{2+}-dependent manner, suggesting a conserved reaction to binding of the EF-hand domains to Ca^{2+}. Translocation of repair-mediating factors to the wound site in response to a local increase of Ca^{2+} is common in different plasma membrane repair models. For example, in injured human myotubes, calpain, a Ca^{2+}-dependent cysteine protease, which acts as a primary mediator of membrane repair, rapidly accumulates at the site of injury (Redpath *et al.* 2014). Similarly, membrane-binding annexins, which mediate wound sealing through vesicle fusion, aggregate at wound sites in different types of mammalian cells (Carmeille *et al.* 2016; Koerdt and Gerke 2017). This quick activation and translocation of preformed proteins allows a very rapid response independent of time-consuming gene transcription or protein biosynthesis, which an injured cell cannot afford. Our data demonstrate that in fungi PEF1 belongs to these preformed response factors.

The rapidly increasing intracellular Ca^{2+} concentration at the wound site has mostly been attributed to the influx of extracellular Ca^{2+}. Similar to other eukaryotic organisms, fungi maintain a low cytosolic Ca^{2+} concentration and higher concentrations of this ion in the extracellular space or within organelles [reviewed in Cyert and Philpott (2013)]. Disintegration of the plasma membrane therefore quickly results in collapsing of this gradient and local cytoplasmic Ca^{2+} increase. When in our study calcium was reduced or depleted in the growth medium, recruitment of PEF1 to the plasma membrane in response to injury was significantly reduced, fully consistent with these current models of membrane repair. A recent study investigating sarcolemma repair in murine muscle fibers also identified lysosomal Ca^{2+} as an essential intracellular source during Ca^{2+}-mediated membrane injury responses (Cheng *et al.* 2014). Since a lack of Ca^{2+} in the growth medium can also result in depletion of intracellular Ca^{2+} storages, we cannot exclude the possibility that also the cytoplasmic increase in Ca^{2+} through influx from organelles, such as vacuoles, might control PEF1 dynamics. A more detailed understanding of the Ca^{2+} fluxes throughout healthy and injured fungal cells will be a vital

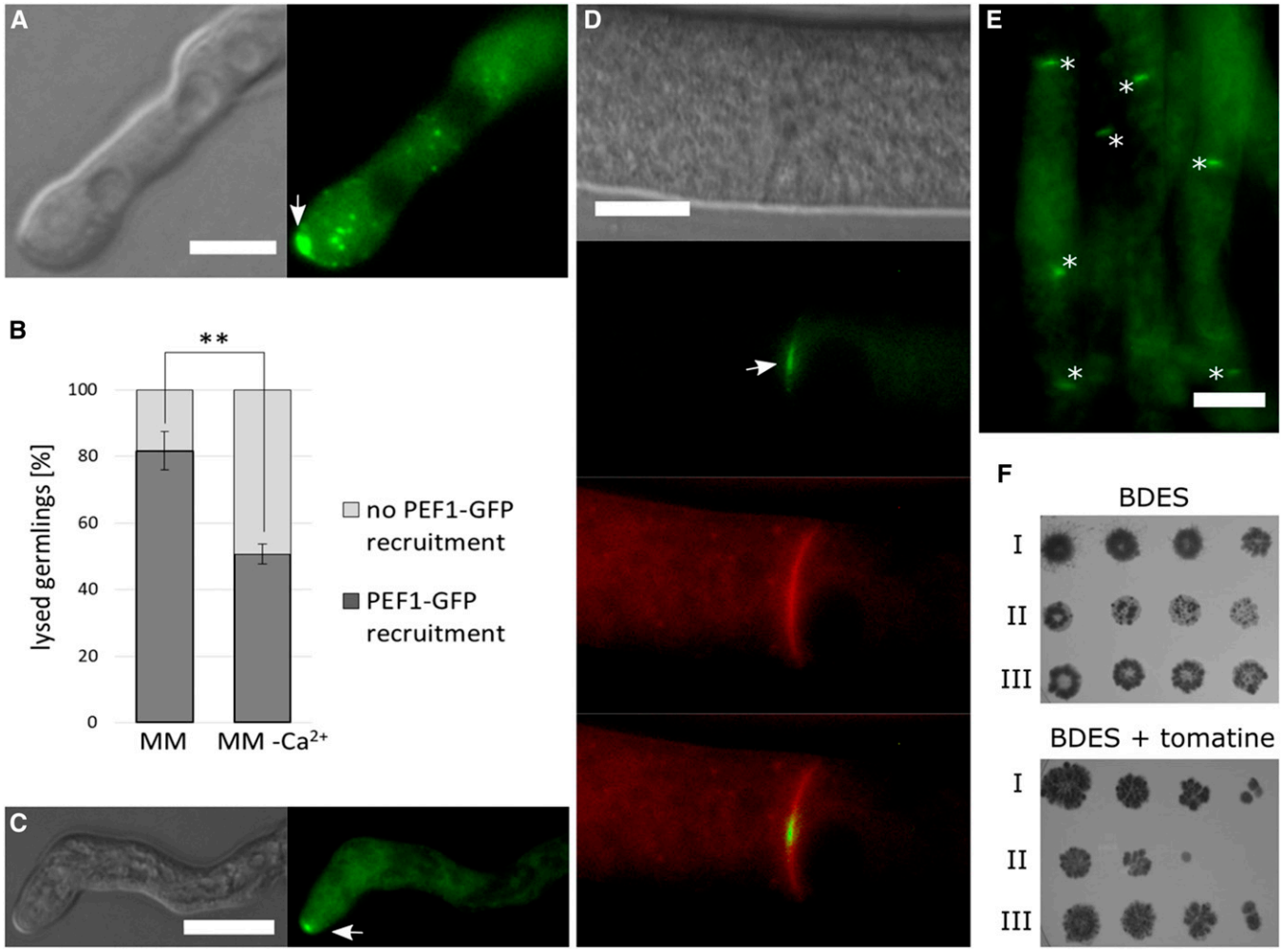

Figure 6 PEF1-GFP is recruited in response to tomatine-induced cell lyses and contributes to the survival in presence of this pore-forming drug. (A) Recruitment of PEF1-GFP to the germling tips in response to tomatine-induced cell lysis (arrow). Left: DIC; right: GFP fluorescence. Bar, 5 μm. (B) Quantification of PEF1-GFP recruitment in germlings treated with tomatine on MM and MM without Ca^{2+}. Error bars indicate the SD calculated from three independent experiments (n = 100 each). The asterisks represent statistically significant differences determined by the Student's t-test (**$P \leq$ 0.01). (C) Recruitment of PEF1-GFP to a tip of a mature hypha in response to tomatine-induced cell lysis (arrow). Left: DIC; right: GFP fluorescence. (D) PEF1-GFP recruitment to the septal pore (arrow) after treatment with tomatine in mature hypha. The plasma membrane was stained in red with the lipophilic dye FM4-64. Top image: DIC; second image from top: GFP; third image from the top: FM4-64; bottom image: merger of GFP and FM4-64 images. (E) Overview of a group of hyphae exhibiting PEF1-GFP at septal pores after tomatine treatment (aggregates indicated by asterisks). (A–E) Strain GN9-22 (*Ptef-1-pef-1-gfp*). Bars in (A–E), 10 μm. (F) Fivefold serial spore dilutions (10^5–10^2) of wild type (I) (FGSC 988), Δ*pef1* (II) (FGSC 15890), and the complemented strain Δ*pef1 Ptef-1-pef1-gfp* (III) (GN9-22) were spotted on BDES medium and on BDES medium containing 75 μg/ml tomatine. Growth was documented after 3 dpi.

prerequisite for fully understanding membrane repair in this group of organisms.

PEF1 mediates protection against membrane fusion-induced cell lysis

The loss of *pef1* results in increased fusion-induced lysis only in lysis-prone mutants but not in a wild-type background. This observation suggests that in the wild type, cell fusion is robust and repair mechanisms are dispensable. In the Δ*Prm1* and Δ*lfd-1* mutants, however, the onset of plasma membrane fusion has three different outcomes. First, cell pairs fuse in a wild-type like manner. Second, the fusion process arrests after cell wall deconstruction, and third, the cells lyse because of membrane rupture. Cell lysis is strongly correlated to the moment of cytoplasmic mixing, suggesting that lysis is caused by the engagement of the cell fusion machinery. So far the molecular functions of PRM1 and LFD-1 remain unknown. They appear to ensure fusion fidelity, probably by organizing or spatially restricting the fusion machinery (Fleissner *et al.* 2009; Palma-Guerrero *et al.* 2014). The lack of LFD-2 or FIG1 also causes increased lysis rates, but no adhering membranes are observed, indicating distinct functions from PRM1 and LFD-1 (Palma-Guerrero *et al.* 2015). Interestingly, the lysis rates in Δfig1 do not further increase in the absence of *pef1*. FIG1 is a low affinity Ca^{2+} uptake system, facilitating Ca^{2+} influx, which is mediating mating fusion in *S. cerevisiae* and *C. albicans* (Muller *et al.*

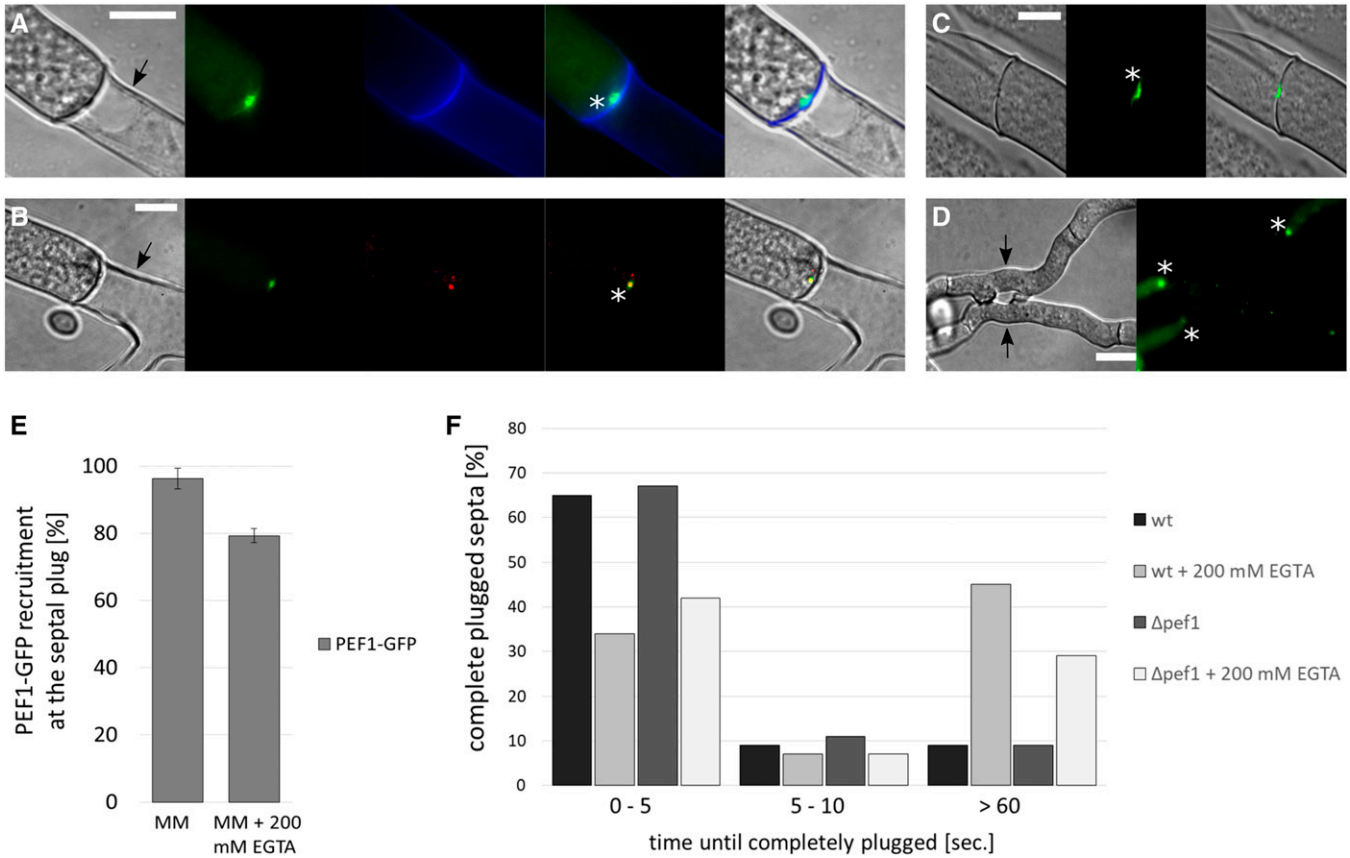

Figure 7 PEF1-GFP localizes to the septal plug after injury and during programmed cell death. (A) PEF1-GFP recruitment to the septal pore after cutting of the hypha with a laser (strain GN3-17, *Pccg-1-pef-1-gfp*). Arrow: injured, empty compartment. Asterisk indicates the septal plug. The cell wall was stained with the chitin-binding dye calcofluor white (CFW, 100 μg/ml) (false colored in blue). Images from the left: (1) DIC; (2) GFP fluorescence; (3) CFW; (4) merged image of GFP and CFW; (5) merged image of 1–3. (B) Co-localization of PEF1-GFP and the Woronin body, which is visualized by dsRED-HEX-1, in a heterokaryon of strains S10 (*Pccg-1-pef-1-gfp*) and S20 (*Pccg-1-dsred-hex-1*). The asterisk indicates the septal plug, the arrow the injured compartment. Images from the left: (1) DIC; (2) GFP fluorescence; (3) dsRED fluorescence; (4) merged image of GFP and dsRED; (5) merged image of 1–3. (C) Recruitment of PEF1-GFP to the septal pore in the Δ*hex-1* strain (S48, *Pccg-1-pef-1-gfp*), which does not possess Woronin bodies, after cutting the hypha with a laser. The asterisk indicates the septal plug. Left: DIC; center: GFP; right: merged image of DIC and GFP. (D) PEF1-GFP recruitment to septal plugs in hyphae undergoing programmed cell death induced by heterokaryon incompatibility [forced heterokaryon of C9-15 and GN3-36 (*Pccg-1-pef-1-gfp*)]. Arrows indicate compartments undergoing cell death. Asterisks indicate septal plugs. Note the absence of GFP fluorescence in the dead compartments. Left: DIC; right: GFP. Bar, 10 μm (A–D). (E) Quantification of PEF1-GFP recruitment to the septal plug after cutting with a laser on MM and MM + 200 mM EGTA (strain GN3-17, *Pccg-1-pef-1-gfp*). Error bars indicate the SD calculated from three independent experiments (n = 100 each). (F) Comparison of the time required for complete sealing of the septal pore in the wild type (FGSC 988) and the Δ*pef1* strain (FGSC 15890) on MM and MM + 200 mM EGTA. Two hundred hyphae of each strain were cut with a laser and the time until cytoplasmic leakage through the septal pore ceased was measured.

2003; Yang *et al.* 2011). While PRM1, LFD-1, and LFD-2 are involved in fusion pore formation, FIG1 might play a role in an earlier step of the fusion process, before engagement of the fusion machinery. The observed cell lysis in Δfig1 might not be caused by fusion-induced membrane rupture and might therefore not activate the PEF1-mediated response. Studying the interplay of the different fusion factors and also the related membrane repair mechanisms in *N. crassa* represents one very promising strategy to further illuminate the molecular mechanisms mediating eukaryotic cell–cell fusion.

PEF1 appears to function independently of the ESCRT-III complex

While our data strongly support a role of PEF1 in mediating the response to different types of membrane injuries in fungi, the exact molecular repair mechanisms remain unknown. In mammalian muscle cells, the PEF1 homologous ALG-2 accumulates at membrane injury sites in a Ca^{2+}-dependent manner and acts as an initiator of ALIX recruitment and ESCRT-III–Vps4 complex formation. As a consequence, the injured membrane region undergoes shedding and repair (Scheffer *et al.* 2014). While the involved proteins are conserved in fungi, our data suggest that in *N. crassa*, PEF1 functions in an ESCRT-III-independent way. No recruitment of the ESCRT proteins to the plasma membrane or co-localization with PEF1 was observed. In addition to its interaction with the ESCRT complex, ALG-2 and homologous proteins are involved in various different cellular processes, including ER-to-Golgi vesicular transport or signal transduction from the membrane to downstream

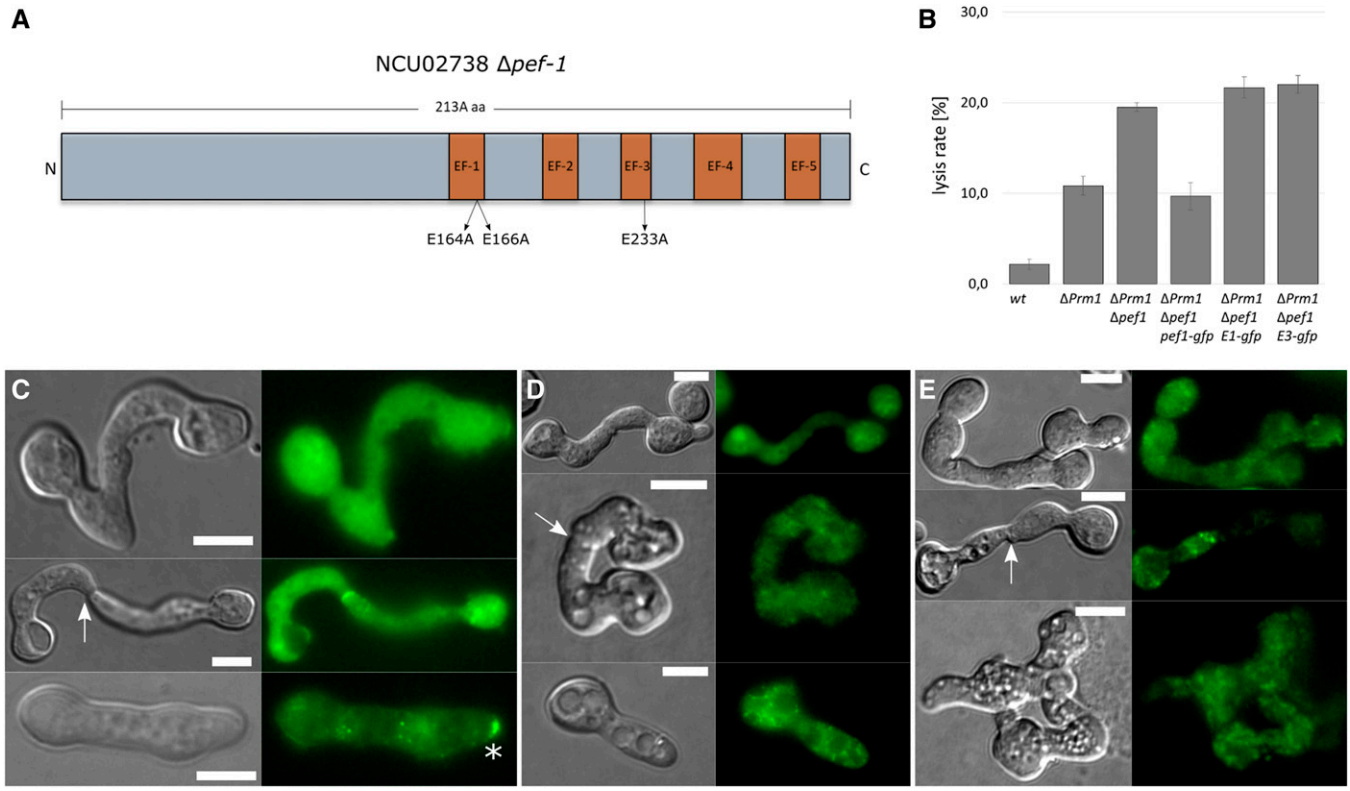

Figure 8 The EF-hand domains EF-1 and EF-3 are essential for PEF1 function. (A) Cartoon illustrating the structure of PEF1. The five EF-Hand domains and their relative positions are highlighted in orange. The replaced amino acids in EF-1 and EF-3 are indicated. (B) Quantification of the lysis rate during germling fusion in the Δ*Prm1*/Δ*pef1* strains expressing *pef1-gfp* (GN7-54), *pef1*$^{E164A/E166A}$*-gfp* (GN9-34), and *pef1*^{E233A}*-gfp* (GN9-1). The wild type (FGSC 988) and Δ*Prm1* (A32) were used as controls. Error bars indicate the SD calculated from three independent experiments (n = 100 each). Localization of (C) PEF1-GFP [GN9-22 (*Ptef-1-pef-1-gfp*)], (D) PEF1$^{E164A/E166A}$-GFP [GN9-34 (*Ptef-1-pef-1*$^{E164A/E166A}$*-gfp*)], and (E) PEF1^{E233A}-GFP [GN9-1 (*Ptef-1-pef-1*^{E233A}*-gfp*)] during successful fusion (top), fusion failure (middle), and during nystatin-induced cell lysis (bottom). The arrows point to the fusion point and the asterisk indicates PEF1 aggregates at the plasma membrane. Left images: DIC; right images: GFP. Bar, 5 μm.

factors [reviewed in Maki *et al.* (2016)]. It is therefore conceivable that an ESCRT-III independent membrane repair mechanism is controlled by PEF1. Fungal PEF1 shares only homology with ALG-2 in the C-terminal two-thirds of the protein. The N-terminal third is specific for fungi. This part might mediate the interaction with other, probably fungal-specific, proteins. An attractive hypothesis is that PEF1 might serve as a conserved upstream sensor of membrane injury mediating divergent downstream molecular processes. The potential existence of fungal-specific membrane repair mechanisms calls for further investigation, since they might provide highly interesting targets for controlling fungi. An earlier study identified the synaptotagmin SYT1 as part of a fungal membrane repair mechanism (Palma-Guerrero *et al.* 2014). Similar to our observations for *pef1*, the introduction of the *syt1* knockout mutation in lysis-prone fusion mutants significantly increased the number of lysing cell fusion pairs. In our hands, however, the *syt1* double mutants did not show this defect, suggesting that this phenotype is not robust. We hypothesize that different culture conditions, which could not be controlled for, resulted in the contradictory observations in the two studies.

Membrane repair could contribute to antifungal resistance

PEF1 accumulates at the plasma membrane during exposure to pore-forming drugs, and the lack of PEF1 results in an increased sensitivity to the plant defense compound tomatine. Plants possess two lines of chemical antimicrobial defense. First, numerous species accumulate preformed antifungals or phytoanticipines, such as the glycoalkaloids of nightshades including tomatine. Second, many plants produce defense compounds in response to an infection, so called phytoalexins. Both phytoanticipins and phytoalexins include pore-forming substances (Osbourn 1999). The current model of fungal resistance against plant defense compounds and antifungals includes two different mechanisms, which function in a step-wise manner: first, the activation of efflux pumps, which reduce the intracellular concentration of the toxic chemicals; and second, the enzymatic degradation of these compounds (Denny and VanEtten 1981, 1983; Fleissner *et al.* 2002). The gene expression of efflux pumps is induced within minutes after toxin exposure, allowing rapid protection and providing time for activation of the detoxification response (Del Sorbo *et al.* 2000; Fleissner *et al.* 2002). The main caveat of this model is, however, still a "time conundrum": although the

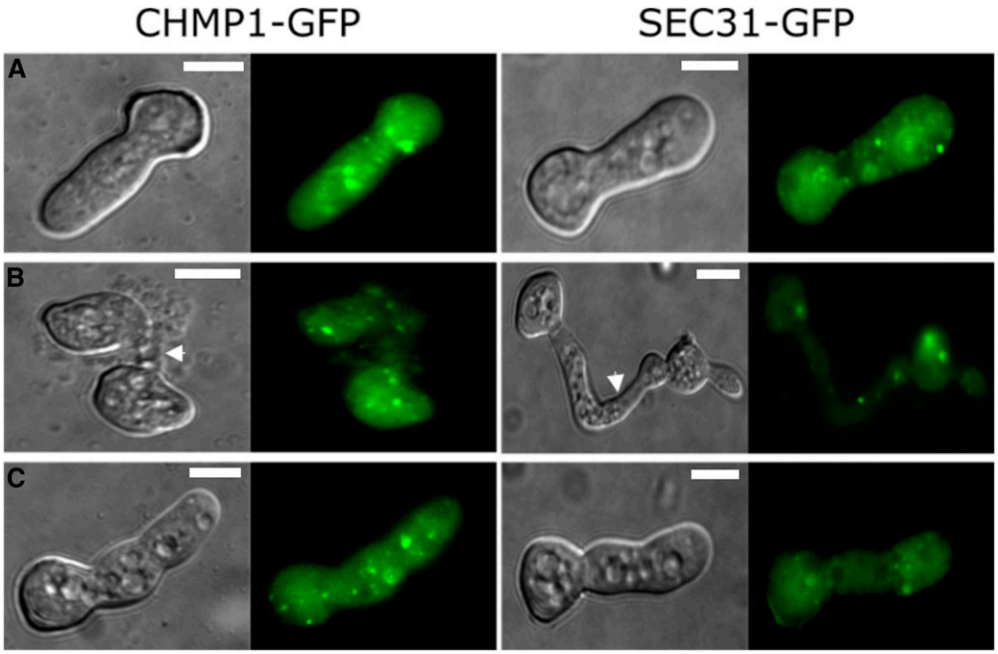

Figure 9 The ESCRT-III complex proteins CHMP1-GFP and SEC31-GFP do not accumulate at the plasma membrane during fusion-induced lysis or after nystatin treatment. Subcellular localization of CHMP1-GFP (GN9-50) and SEC31-GFP (GN9-48) in untreated healthy germlings (A), during fusion failure (B), and during nystatin-induced cell lysis (C). Fusion points are indicated (arrows). Left images: DIC; right images: GFP. Bar, 5 μm.

activation of efflux pumps is rapid, it might not be fast enough. Once a pore-forming drug is interacting with membrane lipids, the lipid bilayer is disintegrating, and the cell would quickly die. Based on our data, we suggest adding a third line of defense into the current model. We hypothesize that membrane repair mechanisms provide instant protection against pore-forming drugs, even before efflux pumps are activated. The model therefore comprises three successive steps: (1) Membrane repair, (2) Efflux, and (3) Detoxification. Since important clinical antifungals also target the plasma membrane, this model might also apply to the fungal cellular response against these drugs. It will be of great interest to test this hypothesis in clinically and agriculturally relevant fungal species.

Interestingly, we did not observe an increased sensitivity of the Δ*pef1* mutant to the polyene nystatin. Nystatin and tomatine are both pore-forming drugs and PEF1-GFP accumulated at the membrane after treatment with both substances, albeit to a lesser extent during nystatin application. So far, this difference is inconceivable. Our data support the notion that other membrane repair mechanisms exist in *N. crassa*, with partially overlapping functions with the PEF1 pathway. If the spatial and/or temporal dynamics of the membrane injuries caused by tomatine and nystatin differ, the different repair mechanisms might have different contributions, which could explain the observed differences. Also, if the nystatin treatment results in a significantly lower Ca^{2+} influx than the tomatine treatment, repair mechanisms might not be sufficiently activated to prevent cell death. This hypothesis is supported by the marked weaker PEF1 recruitment to the plasma membrane in response to nystatin compared to tomatine. In human cells, two annexins with different Ca^{2+} sensitivities mediate specific responses to different types of injuries (Potez *et al.* 2011). Similarly, PEF1 might be more sensitive to Ca^{2+} than the so far unknown repair mechanism required to cope with nystatin-induced injuries. This could explain why a recruitment of PEF1 to the plasma membrane in response to nystatin was observed but no changes in the nystatin sensitivity of the Δ*pef1* mutant were detected. Therefore, identifying the complete set of repair machineries, their interplay, and their activation modes will be of high relevance for fully understanding and controlling the cellular response to membrane-targeting antifungal drugs.

PEF1 is involved in the clogging of septal pores

PEF1 accumulates at septal pores in response to tomatine exposure. Similarly, the protein is part of the pore plug formed after hyphal transsection. While the occlusion of septal pores by Woronin bodies has already been described in the early days of mycology (Buller 1933), recent years have seen the identification of numerous proteins accumulating not only around the Woronin body, but also in Woronin body-independent pore occlusions (Fleissner and Glass 2007; Lai *et al.* 2012). The first protein identified to take place in these processes was the SO protein of *N. crassa*, which shows comparable dynamics to PEF1 (Fleissner and Glass 2007). A common characteristic of pore-occluding proteins is stretches of disordered structure (Lai *et al.* 2012). The fungal-specific N-terminal first third of PEF1 is meeting this requirement. It is likely that pore occlusion has evolved as a secondary role of proteins with different primary functions. The SO protein, for example, is involved in the signaling of fungal germlings and hyphae undergoing vegetative cell fusion (Fleissner *et al.* 2005). The aggregation of proteins at the septal pore promotes its closure through the Woronin body by a sealing mechanism. In Woronin body-independent septal pore sealing, *e.g.*, during vegetative incompatibility or hyphal aging, the proteinous aggregates even seem to serve as the main

plug for hyphal compartmentation (Fleissner *et al.* 2005; Lai *et al.* 2012). The recruitment of PEF1 to basically all septa within a hyphal network after exposure to tomatine might hint to an important mechanism employed by fungi to control their multicellular state. Fungal multicellularity has evolved independently of plant and animal tissues. So far, the functioning and adaptation of multicellular fungal colonies is only very poorly understood. Healthy hyphae of *N. crassa* are a syncytium, growing by tip extension and branching. While hyphal differentiation includes permanent compartmentation by septal pore plugging, there is evidence that pores can also be closed temporarily (Markham 1994; Bleichrodt *et al.* 2012). PEF1 might provide a suitable marker for further investigation of the still poorly understood functioning of multicellular fungal colonies.

Acknowledgments

We thank Ralf Schnabel and Christian Hennig for ongoing support in developing our microscopy. We are grateful to Ulrich Kück and Ines Teichert for hosting C.A. for laser dissection experiments. We thank Louise Glass and Javier Palma-Guerrero for providing various mutant strains. We gratefully acknowledge use of materials generated by PO1 GM068087, "Functional analysis of a model filamentous fungus." This work was in part supported by funding from the German Research Foundation (Grants FL706/1-1 and FL706/1-2) to A.F.

Literature Cited

Aguilar, P. S., A. Engel, and P. Walter, 2007 The plasma membrane proteins Prm1 and Fig1 ascertain fidelity of membrane fusion during yeast mating. Mol. Biol. Cell 18: 547–556. https://doi.org/10.1091/mbc.e06-09-0776

Babiychuk, E. B., K. Monastyrskaya, S. Potez, and A. Draeger, 2011 Blebbing confers resistance against cell lysis. Cell Death Differ. 18: 80–89. https://doi.org/10.1038/cdd.2010.81

Barthélémy, F., A. Defour, N. Levy, M. Krahn, and M. Bartoli, 2018 Muscle cells fix breaches by orchestrating a membrane repair ballet. J. Neuromuscul. Dis. 5: 21–28. https://doi.org/10.3233/JND-170251

Berepiki, A., A. Lichius, J. Y. Shoji, J. Tilsner, and N. D. Read, 2010 F-actin dynamics in *Neurospora crassa*. Eukaryot. Cell 9: 547–557. https://doi.org/10.1128/EC.00253-09

Bleichrodt, R. J., G. J. van Veluw, B. Recter, J. Maruyama, K. Kitamoto *et al.*, 2012 Hyphal heterogeneity in *Aspergillus oryzae* is the result of dynamic closure of septa by Woronin bodies. Mol. Microbiol. 86: 1334–1344. https://doi.org/10.1111/mmi.12077

Bolard, J., 1986 How do the polyene macrolide antibiotics affect the cellular membrane properties? Biochim. Biophys. Acta 864: 257–304. https://doi.org/10.1016/0304-4157(86)90002-X

Brockman, H. E., and F. J. De Serres, 1963 Sorbose toxicity in neurospora. Am. J. Bot. 50: 709–714. https://doi.org/10.1002/j.1537-2197.1963.tb12246.x

Buller, A., 1933 *Researches on Fungi*. Longman, London.

Cano-Domínguez, N., K. Alvarez-Delfin, W. Hansberg, and J. Aguirre, 2008 NADPH oxidases NOX-1 and NOX-2 require the regulatory subunit NOR-1 to control cell differentiation and growth in *Neurospora crassa*. Eukaryot. Cell 7: 1352–1361. https://doi.org/10.1128/EC.00137-08

Carmeille, R., F. Bouvet, S. Tan, C. Croissant, C. Gounou *et al.*, 2016 Membrane repair of human skeletal muscle cells requires Annexin-A5. Biochim. Biophys. Acta 1863: 2267–2279. https://doi.org/10.1016/j.bbamcr.2016.06.003

Chandrasekar, P., 2011 Management of invasive fungal infections: a role for polyenes. J. Antimicrob. Chemother. 66: 457–465. https://doi.org/10.1093/jac/dkq479

Cheng, X., X. Zhang, Q. Gao, M. Ali Samie, M. Azar *et al.*, 2014 The intracellular Ca^{2+} channel MCOLN1 is required for sarcolemma repair to prevent muscular dystrophy. Nat. Med. 20: 1187–1192. https://doi.org/10.1038/nm.3611

Clarke, M. S., R. W. Caldwell, H. Chiao, K. Miyake, and P. L. McNeil, 1995 Contraction-induced cell wounding and release of fibroblast growth factor in heart. Circ. Res. 76: 927–934. https://doi.org/10.1161/01.RES.76.6.927

Colot, H. V., G. Park, G. E. Turner, C. Ringelberg, C. M. Crew *et al.*, 2006 A high-throughput gene knockout procedure for Neurospora reveals functions for multiple transcription factors. Proc. Natl. Acad. Sci. USA 103: 10352–10357 (erratum: Proc. Natl. Acad. Sci. USA 103: 16614). https://doi.org/10.1073/pnas.0601456103

Cyert, M. S., and C. C. Philpott, 2013 Regulation of cation balance in *Saccharomyces cerevisiae*. Genetics 193: 677–713. https://doi.org/10.1534/genetics.112.147207

Dal Peraro, M., and F. G. van der Goot, 2016 Pore-forming toxins: ancient, but never really out of fashion. Nat. Rev. Microbiol. 14: 77–92. https://doi.org/10.1038/nrmicro.2015.3

Daskalov, A., J. Heller, S. Herzog, A. Fleißner, and N. L. Glass, 2016 Molecular mechanisms regulating cell fusion and heterokaryon formation in filamentous fungi. Microbiol. Spectr. 5. https://doi.org/10.1128/microbiolspec.FUNK-0015-2016

Davenport, N. R., and W. M. Bement, 2016 Cell repair: revisiting the patch hypothesis. Commun. Integr. Biol. 9: e1253643. https://doi.org/10.1080/19420889.2016.1253643

Del Sorbo, G., H. Schoonbeek, and M. A. De Waard, 2000 Fungal transporters involved in efflux of natural toxic compounds and fungicides. Fungal Genet. Biol. 30: 1–15. https://doi.org/10.1006/fgbi.2000.1206

Denny, T. P., and H. D. VanEtten, 1981 Tolerance by *Nectria haematococca* M P VI of the chickpea (*Cicer arietinum*) phytoalexins medicarpin and maackiain. Physiol. Plant Pathol. 19: 419–437. https://doi.org/10.1016/S0048-4059(81)80073-2

Denny, T. P., and H. D. VanEtten, 1983 Tolerance of *Nectria haematococca* MP VI to the phytoalexin pisatin in the absence of detoxification. J. Gen. Microbiol. 129: 2893–2901.

Dunlap, J. C., K. A. Borkovich, M. R. Henn, G. E. Turner, M. S. Sachs *et al.*, 2007 Enabling a community to dissect an organism: overview of the Neurospora functional genomics project. Adv. Genet. 57: 49–96. https://doi.org/10.1016/S0065-2660(06)57002-6

Eddleman, C. S., G. D. Bittner, and H. M. Fishman, 2000 Barrier permeability at cut axonal ends progressively decreases until an ionic seal is formed. Biophys. J. 79: 1883–1890. https://doi.org/10.1016/S0006-3495(00)76438-1

Eilam, Y., and N. Grossowicz, 1982 Nystatin effects on cellular calcium in *Saccharomyces cerevisiae*. Biochim. Biophys. Acta 692: 238–243. https://doi.org/10.1016/0005-2736(82)90527-2

Elias, P. M., D. S. Friend, and J. Goerke, 1979 Membrane sterol heterogeneity. Freeze-fracture detection with saponins and filipin. J. Histochem. Cytochem. 27: 1247–1260. https://doi.org/10.1177/27.9.479568

Fleissner, A., and N. L. Glass, 2007 SO, a protein involved in hyphal fusion in *Neurospora crassa*, localizes to septal plugs. Eukaryot. Cell 6: 84–94. https://doi.org/10.1128/EC.00268-06

Fleissner, A., C. Sopalla, and K. M. Weltring, 2002 An ATP-binding cassette multidrug-resistance transporter is necessary for tolerance of *Gibberella pulicaris* to phytoalexins and virulence on potato tubers. Mol. Plant Microbe Interact. 15: 102–108. https://doi.org/10.1094/MPMI.2002.15.2.102

Fleissner, A., S. Sarkar, D. J. Jacobson, M. G. Roca, N. D. Read *et al.*, 2005 The so locus is required for vegetative cell fusion and postfertilization events in *Neurospora crassa*. Eukaryot. Cell 4: 920–930. https://doi.org/10.1128/EC.4.5.920-930.2005

Fleissner, A., S. Diamond, and N. L. Glass, 2009 The *Saccharomyces cerevisiae* PRM1 homolog in *Neurospora crassa* is involved in vegetative and sexual cell fusion events but also has postfertilization functions. Genetics 181: 497–510. https://doi.org/10.1534/genetics.108.096149

Freitag, M., P. C. Hickey, N. B. Raju, E. U. Selker, and N. D. Read, 2004 GFP as a tool to analyze the organization, dynamics and function of nuclei and microtubules in *Neurospora crassa*. Fungal Genet. Biol. 41: 897–910. https://doi.org/10.1016/j.fgb.2004.06.008

Friedman, M., 2002 Tomato glycoalkaloids: role in the plant and in the diet. J. Agric. Food Chem. 50: 5751–5780. https://doi.org/10.1021/jf020560c

Glass, N. L., and I. Kaneko, 2003 Fatal attraction: nonself recognition and heterokaryon incompatibility in filamentous fungi. Eukaryot. Cell 2: 1–8. https://doi.org/10.1128/EC.2.1.1-8.2003

Heiman, M. G., and P. Walter, 2000 Prm1p, a pheromone-regulated multispanning membrane protein, facilitates plasma membrane fusion during yeast mating. J. Cell Biol. 151: 719–730. https://doi.org/10.1083/jcb.151.3.719

Horn, A., and J. K. Jaiswal, 2018 Cellular mechanisms and signals that coordinate plasma membrane repair. Cell. Mol. Life Sci. 75: 3751–3770. https://doi.org/10.1007/s00018-018-2888-7

Howard, A. C., A. K. McNeil, F. Xiong, W. C. Xiong, and P. L. McNeil, 2011 A novel cellular defect in diabetes: membrane repair failure. Diabetes 60: 3034–3043. https://doi.org/10.2337/db11-0851

Idone, V., C. Tam, and N. W. Andrews, 2008a Two-way traffic on the road to plasma membrane repair. Trends Cell Biol. 18: 552–559. https://doi.org/10.1016/j.tcb.2008.09.001

Idone, V., C. Tam, J. W. Goss, D. Toomre, M. Pypaert *et al.*, 2008b Repair of injured plasma membrane by rapid Ca^{2+}-dependent endocytosis. J. Cell Biol. 180: 905–914. https://doi.org/10.1083/jcb.200708010

Jedd, G., and N. H. Chua, 2000 A new self-assembled peroxisomal vesicle required for efficient resealing of the plasma membrane. Nat. Cell Biol. 2: 226–231. https://doi.org/10.1038/35008652

Jin, H., C. Carlile, S. Nolan, and E. Grote, 2004 Prm1 prevents contact-dependent lysis of yeast mating pairs. Eukaryot. Cell 3: 1664–1673. https://doi.org/10.1128/EC.3.6.1664-1673.2004

Kinsky, S. C., 1961 Alterations in the permeability of *Neurospora crassa* due to polyene antibiotics. J. Bacteriol. 82: 889–897.

Koerdt, S. N., and V. Gerke, 2017 Annexin A2 is involved in Ca^{2+}-dependent plasma membrane repair in primary human endothelial cells. Biochim Biophys Acta Mol Cell Res 1864: 1046–1053. https://doi.org/10.1016/j.bbamcr.2016.12.007

la Cour, J. M., P. Winding Gojkovic, S. E. B. Ambjorner, J. Bagge, S. M. Jensen *et al.*, 2018 ALG-2 participates in recovery of cells after plasma membrane damage by electroporation and digitonin treatment. PLoS One 13: e0204520. https://doi.org/10.1371/journal.pone.0204520

Lai, J., C. H. Koh, M. Tjota, L. Pieuchot, V. Raman *et al.*, 2012 Intrinsically disordered proteins aggregate at fungal cell-to-cell channels and regulate intercellular connectivity. Proc. Natl. Acad. Sci. USA 109: 15781–15786. https://doi.org/10.1073/pnas.1207467109

Maki, M., T. Takahara, and H. Shibata, 2016 Multifaceted roles of ALG-2 in Ca(2+)-regulated membrane trafficking. Int. J. Mol. Sci. 17.

Margolin, B. S., M. Freitag, and E. U. Selker, 1997 Improved plasmids for gene targeting at the *his-3* locus of *Neurospora crassa* by electroporation. Fungal Genet. Newsl. 44: 34–36.

Markham, P., 1994 Occlusions of septal pores in filamentous fungi. Mycol. Res. 98: 1089–1106. https://doi.org/10.1016/S0953-7562(09)80195-0

McNeil, P. L., and R. Khakee, 1992 Disruptions of muscle fiber plasma membranes. Role in exercise-induced damage. Am. J. Pathol. 140: 1097–1109.

McNeil, P. L., and T. Kirchhausen, 2005 An emergency response team for membrane repair. Nat. Rev. Mol. Cell Biol. 6: 499–505. https://doi.org/10.1038/nrm1665

Mondal, A. K., A. Sreekumar, N. Kundu, R. Kathuria, P. Verma *et al.*, 2018 Structural basis and functional implications of the membrane pore-formation mechanisms of bacterial pore-forming toxins. Adv. Exp. Med. Biol. 1112: 281–291. https://doi.org/10.1007/978-981-13-3065-0_19

Muller, E. M., N. A. Mackin, S. E. Erdman, and K. W. Cunningham, 2003 Fig1p facilitates Ca^{2+} influx and cell fusion during mating of *Saccharomyces cerevisiae*. J. Biol. Chem. 278: 38461–38469. https://doi.org/10.1074/jbc.M304089200

Nakamura, M., A. N. M. Dominguez, J. R. Decker, A. J. Hull, J. M. Verboon *et al.*, 2018 Into the breach: how cells cope with wounds. Open Biol. 8. https://doi.org/10.1098/rsob.180135

Osbourn, A. E., 1999 Antimicrobial phytoprotectants and fungal pathogens: a commentary. Fungal Genet. Biol. 26: 163–168. https://doi.org/10.1006/fgbi.1999.1133

Palma-Guerrero, J., C. R. Hall, D. Kowbel, J. Welch, J. W. Taylor *et al.*, 2013 Genome wide association identifies novel loci involved in fungal communication. PLoS Genet. 9: e1003669. https://doi.org/10.1371/journal.pgen.1003669

Palma-Guerrero, J., A. C. Leeder, J. Welch, and N. L. Glass, 2014 Identification and characterization of LFD1, a novel protein involved in membrane merger during cell fusion in *Neurospora crassa*. Mol. Microbiol. 92: 164–182. https://doi.org/10.1111/mmi.12545

Palma-Guerrero, J., J. Zhao, A. P. Goncalves, T. L. Starr, and N. L. Glass, 2015 Identification and characterization of LFD-2, a predicted fringe protein required for membrane integrity during cell fusion in *Neurospora crassa*. Eukaryot. Cell 14: 265–277. https://doi.org/10.1128/EC.00233-14

Potez, S., M. Luginbuhl, K. Monastyrskaya, A. Hostettler, A. Draeger *et al.*, 2011 Tailored protection against plasmalemmal injury by annexins with different Ca^{2+} sensitivities. J. Biol. Chem. 286: 17982–17991. https://doi.org/10.1074/jbc.M110.187625

Rasmussen, C. G., R. M. Morgenstein, S. Peck, and N. L. Glass, 2008 Lack of the GTPase RHO-4 in *Neurospora crassa* causes a reduction in numbers and aberrant stabilization of microtubules at hyphal tips. Fungal Genet. Biol. 45: 1027–1039. https://doi.org/10.1016/j.fgb.2008.02.006

Redpath, G. M., N. Woolger, A. K. Piper, F. A. Lemckert, A. Lek *et al.*, 2014 Calpain cleavage within dysferlin exon 40a releases a synaptotagmin-like module for membrane repair. Mol. Biol. Cell 25: 3037–3048. https://doi.org/10.1091/mbc.e14-04-0947

Riquelme, M., O. Yarden, S. Bartnicki-Garcia, B. Bowman, E. Castro-Longoria *et al.*, 2011 Architecture and development of the *Neurospora crassa* hypha: a model cell for polarized growth. Fungal Biol. 115: 446–474. https://doi.org/10.1016/j.funbio.2011.02.008

Schapire, A. L., V. Valpuesta, and M. A. Botella, 2009 Plasma membrane repair in plants. Trends Plant Sci. 14: 645–652. https://doi.org/10.1016/j.tplants.2009.09.004

Scheffer, L. L., S. C. Sreetama, N. Sharma, S. Medikayala, K. J. Brown *et al.*, 2014 Mechanism of Ca^{2+}-triggered ESCRT

assembly and regulation of cell membrane repair. Nat. Commun. 5: 5646. https://doi.org/10.1038/ncomms6646

Semis, R., I. Polacheck, and E. Segal, 2010 Nystatin-intralipid preparation: characterization and in vitro activity against yeasts and molds. Mycopathologia 169: 333–341. https://doi.org/10.1007/s11046-009-9271-z

Serrano, A., J. Illgen, U. Brandt, N. Thieme, A. Letz *et al.*, 2018 Spatio-temporal MAPK dynamics mediate cell behavior coordination during fungal somatic cell fusion. J. Cell Sci. 131. https://doi.org/10.1242/jcs.213462

Tenney, K., I. Hunt, J. Sweigard, J. I. Pounder, C. McClain *et al.*, 2000 Hex-1, a gene unique to filamentous fungi, encodes the major protein of the Woronin body and functions as a plug for septal pores. Fungal Genet. Biol. 31: 205–217. https://doi.org/10.1006/fgbi.2000.1230

Togo, T., T. B. Krasieva, and R. A. Steinhardt, 2000 A decrease in membrane tension precedes successful cell-membrane repair. Mol. Biol. Cell 11: 4339–4346. https://doi.org/10.1091/mbc.11.12.4339

Tzeng, H. P., S. Evans, F. Gao, K. Chambers, V. K. Topkara *et al.*, 2014 Dysferlin mediates the cytoprotective effects of TRAF2 following myocardial ischemia reperfusion injury. J. Am. Heart Assoc. 3: e000662. https://doi.org/10.1161/JAHA.113.000662

Vernarecci, S., G. Colotti, P. Ornaghi, E. Schiebel, E. Chiancone *et al.*, 2007 The yeast penta-EF protein Pef1p is involved in cation-dependent budding and cell polarization. Mol. Microbiol. 65: 1122–1138. https://doi.org/10.1111/j.1365-2958.2007.05852.x

Vogel, H. J., 1956 A convenient growth medium for Neurospora. Microb. Genet. Bull. 13: 42–46.

Westergaard, M., and H. K. Mitchell, 1947 Neurospora V. A synthetic medium favoring sexual reproduction. Am. J. Bot. 34: 573–577. https://doi.org/10.1002/j.1537-2197.1947.tb13032.x

Xiang, Q., C. Rasmussen, and N. L. Glass, 2002 The *ham-2* locus, encoding a putative transmembrane protein, is required for hyphal fusion in *Neurospora crassa*. Genetics 160: 169–180.

Yang, M., A. Brand, T. Srikantha, K. J. Daniels, D. R. Soll *et al.*, 2011 Fig1 facilitates calcium influx and localizes to membranes destined to undergo fusion during mating in *Candida albicans*. Eukaryot. Cell 10: 435–444. https://doi.org/10.1128/EC.00145-10

Yuan, P., G. Jedd, D. Kumaran, S. Swaminathan, H. Shio *et al.*, 2003 A HEX-1 crystal lattice required for Woronin body function in *Neurospora crassa*. Nat. Struct. Biol. 10: 264–270. https://doi.org/10.1038/nsb910

Communicating editor: M. Freitag